npj | biological physics and mechanics

Review

https://doi.org/10.1038/s44341-025-00020-8

Cellular mechanisms of traumatic brain injury

Gia Kang[1], Eng Kuan Moo[1], Rohan Banton[2], Oren E. Petel[1] & Andrew R. Harris[1]

Mild traumatic brain injury (mTBI) is an acute injury with immediate and medium-term symptom presentation. However, our mechanistic understanding of mTBI and how mechanical loading of soft cellular tissues leads to injury is limited. The aim of this review is to introduce this interdisciplinary field to non-experts and provide an overview of our current understanding of how mechanical trauma contributes to cellular injury. Here, we compare the significance of various measures of mechanical loading including strain magnitude, strain rate, loading mode, and frequency, and their relative significance for cell and tissue injury in *in vitro* and *ex vivo* experimental models reported in the literature. Interestingly, while it is difficult to define a precise injury threshold value based on strain magnitude alone, cellular injury is commonly observed at strain rates of >0.1 s^{-1}, higher than rates observed in many normal cell functions (< 0.01 s^{-1}). We explore the role of the plasma membrane, cytoskeleton, and specialized structures in maintaining cell integrity during traumatic injury.

As part of their normal physiology, cells and tissues undergo changes in shape in response to internally generated and external mechanical forces. For example, adult connective tissues are subjected to mechanical forces as part of everyday movement (such as tendons, skin, muscle etc.), and embryonic epithelial layers are stretched by internally generated forces during formation of the internal organs. In addition to passively sustaining mechanical loads, cells actively sense and respond to mechanical stimuli in their environment through a process referred to as mechano-transduction[1–3]. Cellular responses to load depend greatly on cell type and loading conditions, which can impact cell proliferation[4–6], viability[7–9], and gene expression[10–13]. In addition, mechanical loading of cells and tissues plays an important role in tissue homeostasis. In many connective tissues the absence of mechanical load can lead to tissue degeneration (i.e., muscle atrophy, loss in bone density)[14–16]. Given that sustaining and generating mechanical load is critical for tissue function and homeostasis, many tissues are specialized for this purpose and are composed of extracellular matrix proteins (e.g., collagen, elastin) that are organized into load-bearing structures. In contrast, approximately 80% of the volume of human brain tissue are cells, with a ratio of 5:3:1 for neurons, glia and endothelial cells[17].

Not all mechanical loading of cells and tissues is physiological. Beyond a certain threshold, the amount of deformation or the speed at which a tissue is deformed leads to failure, which can present as symptoms such as tissue rupture[18], haemorrhaging[19], blistering, and cracking[20]. At the cellular level, pathological mechanical loading leads to cell death[21–26] changes in cell morphology[27–29], and subsequently alteration in cell function. What defines the difference between physiological and pathological mechanical loading conditions for a particular tissue, and at what point does this transition occur? This question is significant for both the design of personal protective equipment that aims to attenuate traumatic tissue deformation, and our understanding of the mechanisms of disease. Traumatic brain injury (TBI) provides a relevant example, where impact- or blast-based injuries are caused by excessive brain tissue deformation. Instances of TBI are common, affecting 1153 in every 100,000 individuals per year[30,31] and ranging in severity. Mild traumatic brain injury (mTBI) includes conditions such as concussion, whereas severe traumatic brain injury is characterized by complications such as post-traumatic seizures[32]. mTBI is particularly challenging, as it often goes undiagnosed, but can still lead to long-term medical implications, including Persistent Post-Concussive Symptoms (PPCS). These symptoms, which are developed in approximately 15-25% of mTBI patients[33,34], include chronic headaches, increased likelihood of depression, and dementia[32,35].

While prior studies have primarily explored strain-induced damage at the whole cell and tissue levels, our understanding of the resulting mechanical failure of specific subcellular structures is limited. In this work, we aim to provide an analysis of existing studies to assess our current understanding of injury at the cellular and subcellular levels. Understanding the link between mechanical loading of tissues and the subsequent effect on cellular function requires an interdisciplinary approach that combines concepts from engineering and life sciences. First, we introduce basic measures from mechanical engineering that are commonly used to describe soft tissue deformation. Next, we explore different loading conditions for cells and tissues reported in the literature that are considered physiological

[1]Department of Mechanical and Aerospace Engineering, Carleton University, 1125 Colonel by Drive, Ottawa, ON, K1S 5B6, Canada. [2]U.S. Army Research Laboratory, Aberdeen Proving Ground, Aberdeen, MD, 21005-5066, USA. e-mail: Andrew.harris3@carleton.ca

or pathological. Finally, we focus on traumatic brain injury and explore the effect of different loading conditions has on brain cells by evaluating how different cellular structures respond to mechanical load and under what conditions they are likely to mechanically fail and lead to injury.

Physiological And Pathological Deformations Of Cells And Tissues

Quantitative metrics for characterizing changes in cell and tissue shape

Descriptive, quantitative, and normalized metrics are useful tools for comparing changes in cell and tissue shape and for distinguishing between physiological and pathological loading conditions. Firstly, changes in shape can be characterized by the mode or 'type' of deformation. Cells and tissues experience three primary types of mechanical deformations, namely tension, compression, and shear (see **further reading** and Box 1 for detailed discussion on modes of deformation). Secondly, changes in cell and tissue shape can be quantified by the parameter strain, which measures the amount of deformation. Strain is a second-order tensor that can be represented by a square matrix (e.g., a 3×3 matrix for 3D strain). For example, brain tissue is structurally anisotropic (i.e., direction-dependent) due to structures such as white matter tracts, or nerves. This is observed in mechanical testing data, where *ex vivo* tissue samples from the corpus callosum were measured to be relatively stiffer when tension was applied along the fiber tracts as opposed to in the transverse direction, while they were stiffer in compression applied transverse to the fiber tract directions[36]. It has been suggested that these directional differences are marginal and secondary to anatomical differences seen across various regions in the brain and may therefore be considered mechanically isotropic[36] (i.e., uniform in all directions) in its strain response[36]. However, computational models of head injury have increasingly considered integrating representative tractography to be essential for accurate injury prediction[37–40]. While different physical definitions of strain exist (see Box 1), focusing on a particular mode of strain can provide convenient comparative metrics for studying complex objects such as cells and tissues and are widely used[41–46]. The most commonly used definitions of strain are engineering strain and Green strain. The engineering strain (ε) is used for small deformation ($\varepsilon < 0.01$), whereas Green strain is applicable to a general large deformation. When a deformation becomes too large, cells and tissues can rupture or delaminate leading to cell death. The term 'ultimate strain' defines the strain magnitude value at which failure occurs. Thirdly, as most biological tissues and cells are viscoelastic (a time-dependent material property), strain rate,$\dot{\varepsilon}$, is used to describe the rate at which a given strain magnitude is applied. Finally, many cell types and tissues experience dynamic and repetitive loading conditions, such as a beating heart. Repetitive deformation can be characterized in terms of frequency, which is the number of loading cycles per second (or Hertz). For an example of these values, see Box 2.

Cell and tissue strains

Different strain magnitudes, strain rates, and loading frequencies are observed in diverse cell types and tissues as part of their physiological function. During embryonic development and in processes such as dorsal closure[47,48] and gastrulation[49,50], epithelial sheets can endure large strain magnitudes, up to 0.5–1.0, which typically occur at low strain rates, 10^{-4} to $10^{-3}\ s^{-1}$[51]. In contrast, in adult tissues, strain magnitudes range from 0.1 to 1.0 can occur at high strain rates exceeding $0.1\ s^{-1}$[52–55]. For example, the strain magnitudes associated with cyclic stretching of lungs range between

Box 1 | Strain and Modes of Deformation

Strain is a second order tensor that is usually represented by a square matrix (e.g., a 3×3 matrix for 3D strain). **Tensile** and **compressive** strains are normal strains that act along the surface normal, whereas **shear** strain involves deformation parallel to the surface plane. Normal and shear strains are dimensionless and form the component of a strain matrix. The diagonal components ε_{xx}, ε_{yy} and ε_{zz} of the 3D strain tensor shown below (ε) describe the normal strain in the x-, y- and z-direction respectively, whereas the off-diagonal components $\frac{\gamma_{xy}}{2}$, $\frac{\gamma_{xz}}{2}$ and $\frac{\gamma_{yz}}{2}$ represent shear strain.

$$\varepsilon = \begin{bmatrix} \varepsilon_{xx} & \frac{\gamma_{xy}}{2} & \frac{\gamma_{xz}}{2} \\ \frac{\gamma_{yx}}{2} & \varepsilon_{yy} & \frac{\gamma_{yz}}{2} \\ \frac{\gamma_{zx}}{2} & \frac{\gamma_{zy}}{2} & \varepsilon_{zz} \end{bmatrix}$$

Physical Definitions of Strain

Engineering strain (ε) The normal strain is defined as the ratio of the change in length ($\Delta \mathbf{L} = \mathbf{l} - \mathbf{L}_0$) to the original length of a material $\left(\varepsilon_{yy} = \frac{\Delta L}{L_0}\right)$. The shear component of the engineering strain describes the shape distortion and is defined as $\gamma_{xy} = \frac{\Delta x}{L_0} \approx a$ where Δx indicates the relative displacement between two transverse planes. The engineering strain is suitable for linear elastic materials undergoing small deformation (i.e., length changes that are less than two orders of magnitude of the characteristic length) with negligible rigid body motion.

There are many variants of strain measures developed for different types of loading set-ups. Some of them are defined below based on the uniaxial loading scenario (i.e., normal strain component):

True strain / logarithmic strain (ε_t) The natural logarithm of the ratio of the final length to the original length $\left(\varepsilon_t = \ln\left(\frac{\Delta l}{L_0}\right)\right)$.

This definition accounts for large deformations and is suitable for plastic deformations.

Green strain (ε_G) A strain measure defined with respect to the undeformed (reference) configuration $\left(\varepsilon_G = \frac{1}{2}\left(\frac{l^2 - L_0^2}{L_0^2}\right)\right)$.

This definition is used in finite strain theory and large deformation analysis, along with Almansi strain.

Almansi strain (ε_A) A strain measure defined with respect to the deformed (current) configuration $\left(\varepsilon_A = \frac{1}{2}\left(\frac{l^2 - L_0^2}{l^2}\right)\right)$.

Box 2 | Example values of engineering strain

Example 1: Consider a 90-μm-long section of the axon of a neuron[46] stretched along its long axis and therefore subjected to tensile strain. If the section of the axon undergoes a 4.5 μm extension in 2 seconds, it would experience an engineering strain magnitude of 0.05 μm/μm, sometimes reported as 5%, at a strain rate of $0.025\ s^{-1}$. If this cell underwent cyclic loading, being stretched and then relaxed back to its original shape 10 times in 5 seconds, it undergoes a loading frequency of 2 Hz.

Example 2:

Epithelial cells lining blood vessel walls experience shear strains due to blood flow. Consider a cell with dimensions of 40 μm in length and 5 μm in thickness. If a small shear stress is applied, displacing the top surface of the cell laterally by 0.1 μm relative to the bottom, the cell experiences a shear strain of approximately 0.02 radians, indicating a change of angle by approximately 1.1°.

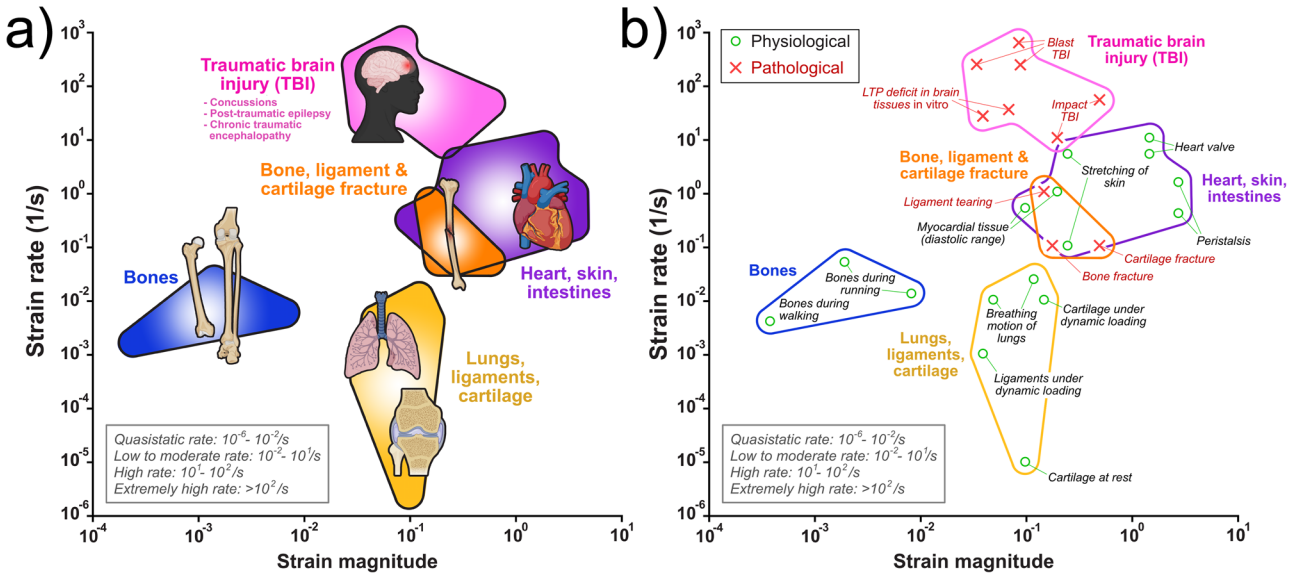

Fig. 1 | Graphical representation of the range of strain loading conditions associated with physiological and pathological processes of the body. a Simplified graphical representation and **b** scatter plot of strain rate versus strain magnitude plot of various physiological and pathological processes. Processes are grouped by the relevant organs and tissues. Values for strain obtained for different tissues including bones[191–195], lungs[56,196,197], ligaments[198,199], and cartilage[200]; brain[61–66,71,72,201], heart[52,57,58,196], skin[55] and intestines[202]. Each point plotted represents the average value from an individual study. The bounding lines are qualitative and are for visual reference only.

0.04–0.12 which occurs at a frequency of 0.2–1 Hz during breathing[56]. Heart valves experience strain magnitudes as high as 1.47[52,57], while diastolic motion of myocardium involves strain magnitudes of 0.1–0.2 and loading frequency of ~1 Hz[58]. Biological tissues often experience a complex combination of deformation modes, strain magnitudes, strain rates, and loading frequencies. A summary of different strain magnitudes and strain rates sustained by selected tissue types is show in Fig. 1.

Transitions from physiological to pathological loading

When strain amplitudes and rates are large, especially for soft tissues that are not specialized for load-bearing, or diseased tissues with attenuated mechanical properties, the applied mechanical loading becomes pathological. A tissue-specific threshold that determines whether a given loading is beneficial or detrimental may exist. We sought to determine the approximate threshold values for strain magnitude and strain rate from the values reported in the literature. When plotting as a function of strain magnitude alone, it is difficult to define a precise injury threshold value although a positive correlation between increasing magnitude and instances of cell injury is both intuitive and seen in the data (Fig. 2a). When plotting as a function of strain rate (Fig. 2b), physiological cellular loading often appears to occur at strain rates <0.01 s^{-1} with many reported pathological loading conditions commonly observed at strain rates of >0.1 s^{-1}. One hypothesis that can be made from this observation is that over this range, some of the cellular structures responsible for maintaining cell shape cannot reorganize to adapt to the deformation occurring on this timescale (for example a strain magnitude of 1.0, at a rate of 0.1 s^{-1}, takes ~10 seconds). To explore this hypothesis, we discuss the different cellular structures important for maintaining brain cell shape in the context of the timescale for their turnover (binding and assembly, un-binding and dis-assembly) and repair, and how strain rates that exceed these limits lead to cellular injury and TBI. While discussing these structures it is important to note that tissue loading *in vivo* is a complex combination of magnitudes and rates in three-dimensional space. Making an estimate of timescale and the turnover of different cellular structures provides a simple starting point for the complex problem of brain tissue injury.

Mechanisms Of Cellular Injury In TBI

Due to the clinical significance of traumatic brain injury, there has been an ongoing effort to estimate the strain magnitudes and strain rates that occur in vivo for brain tissue during impact-based (e.g. collisions during sports) and blast-based (e.g. exposure to explosions) TBI events. There have also been concerted efforts to study TBI in the context of age-related neurodegenerative diseases, as neurodegenerative diseases compromise the brain's structural integrity and resilience, making it more susceptible to traumatic brain injury (TBI) (see, for example, Abdi et al. [59]). In addition, TBI itself can accelerate neurodegenerative processes, creating a cycle of increased vulnerability and progressive cognitive decline (e.g., Brett et al.[60]). Existing studies suggest that the average strain rate experienced by brain tissue during impact TBI could reach as high as 52 s^{-1}. In vitro models and computational simulations of inertia-driven impact TBI have demonstrated that brain tissues deform by peak strain magnitudes of 0.2–0.5 at rates of 10 to 50 s^{-1} [61–70] (Fig. 3a). In blast-driven TBI, computational simulations of the head subjected to shock wave loading predict brain tissue strain magnitude of ≤0.1, but at high rates ranging from 12 to 960 s^{-1}[71,72]. Together, these studies indicate that TBI can occur over a broad range of loading conditions depending on the context of the injury. For the basis of our discussion, we consider mild Traumatic Brain Injury (mTBI) events to occur at a representative average strain magnitude of ~0.3 and strain rate of ~10 s^{-1}.

Cellular responses to high strain rate loading

What happens to the cellular constituents of brain tissue when loaded by a strain magnitude of ~0.3 at a strain rate of ~10 s^{-1} associated with mTBI? Several different cellular structures are well documented as having an important role in sustaining cell shape, which include the plasma membrane, cytoskeleton, cytoplasm as well as a secondary role for some organelles. Furthermore, cells in the brain, such as neurons, often contain specialized structures such as axons, dendrites, and spines that give cells complex morphologies and features that could be damaged during mechanical loading. In general, cellular structures can accommodate changes in cell shape by firstly 'unravelling' or aligning in the direction of mechanical loading (an entropic change), and secondly by 'stretching' which depends on the mechanical properties of the proteins, lipids, and molecules that constitute that structure (an enthalpic change). Cellular structures that can accommodate high strain magnitudes therefore typically either have a lot of 'extra material' that can unravel under stretch or consist of a material that is durable and can stretch without mechanical failure. As part of a living system, many cellular structures undergo active remodelling

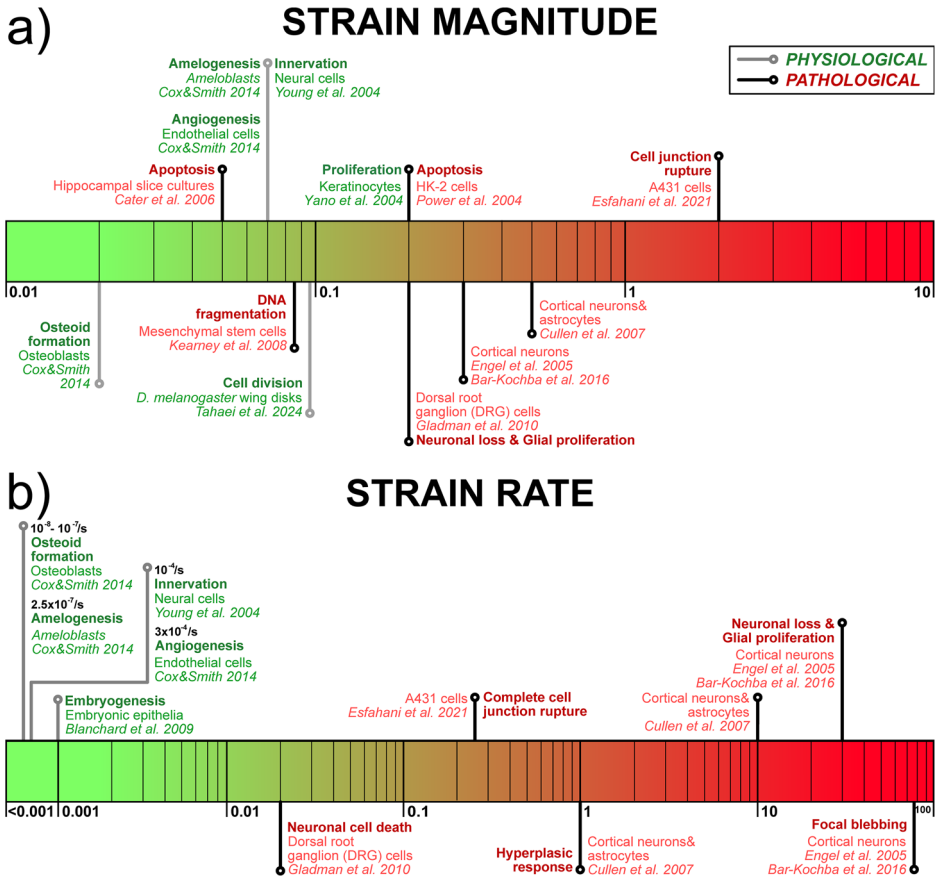

Fig. 2 | Physiological and pathological responses of cells under strain loading. **a** Physiological[203–205] and pathological[21,24,62,126,202,206–208] cellular responses at various strain magnitudes. **b** Physiological[51,204,205] and pathological[21,126,202,207,209] cellular responses at various strain rates. Physiological responses are shown in green text, whereas the pathological responses are shown in red.

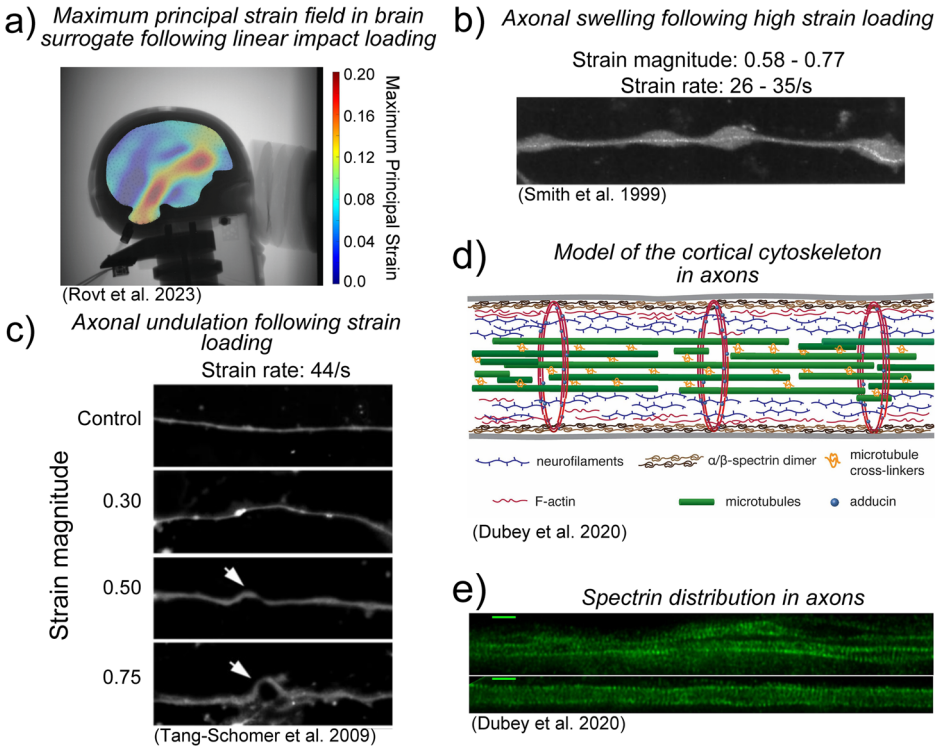

Fig. 3 | Responses of tissue and cellular models of the brain to different strain magnitudes and rates. **a** A representative strain field observed within a head surrogate intended to simulate the brain under mTBI conditions. The strain field was captured at the time point corresponding to the peak maximum principal strain of 0.20 magnitude at rate of 7 s^{-170} (© Rovt et al. 2023, reprinted with permission from Elsevier). **b** Axons show swellings (bulbs) two hours after high strain magnitude, high strain magnitude (0.58–0.77) and high strain rate (26–35 s^{-1})[107] (© Smith et al. 1999, Society for Neuroscience). **c** Degree of axonal undulation is shown to be proportional to the strain amplitude applied at a rate of 44 s^{-142} (© Tang-Schomer et al. 2009, reprinted with permission from Wiley & Sons). **d** Model of the axonal cortical cytoskeleton; The axonal core contains bundled microtubules cross-linked by microtubule-associated proteins. Surrounding this core are neurofilaments and an outer scaffold of periodic F-actin rings connected by α/β-spectrin tetramers aligned along the axon[180] (cross-sections of the tetramers shown as dimers) (Adapted from Dubey et al. 2020, used under CC-BY license). **e** Super-resolution images of axons labelled with anti-βII spectrin (primary) and Alexa Fluor 488 (secondary). Repeated patterns along the axon length indicating ring structures are observed. Scale bar: 1 μm[180] (© Dubey et al. 2020, used under CC-BY license).

and turnover and are repaired as a normal part of cell function. The timescale for critical processes such as protein diffusion, binding, synthesis, and repair, and the timescale over which deformation occurs therefore have complex roles in cellular responses to strain rate.

To study the mechanical response of cells and tissues to external mechanical loading, a range of different tools have been developed. *In vitro* methods for exposing cell cultures and tissues to mechanical stretch are now widely used to evaluate injury in response to deformation[73–77]. In addition to whole cell and tissue loading, biophysical tools such as atomic force microscopy[78,79], micropipette aspiration[80], and optical tweezers[81] can be used to characterize the mechanical properties of subcellular structures, including the properties of cytoskeletal polymers[82–84] and the response of the plasma membrane[85,86]. Similarly, a range of optical microscopy and spectroscopy techniques have been developed to measure the dynamics of proteins and molecules within subcellular structures including single molecule imaging[87,88], Fluorescence Correlation Spectroscopy (FCS)[89,90], and Fluorescence Recovery after Photobleaching (FRAP)[91–94]. In the following sections, we use data reported in the literature that were obtained from whole cell testing, biophysical tools, and microscopy/spectroscopy to make comparisons between the role of strain magnitude, strain rate, and loading frequency on brain cell injury, in the context of a transition from physiological to pathological loading of brain tissue.

Plasma membrane

The plasma membrane separates the interior of mammalian cells from the external environment and consists of a lipid bilayer packed with membrane proteins[95–97]. While lipid bilayers themselves cannot accommodate large planar strains (up to 0.02–0.04[98,99]), the cellular plasma membrane is not flat, and membrane material contained within caveolae (small 50–100 nm membrane invaginations) and other structures can be unravelled under stretch to buffer rapid changes in cellular strain. For example, cells subjected to hypo-osmotic shock, which increases their volume by ~35%, results in a reduction in the number of caveolae by ~30%[100]. In migration of primordial germ cells, membrane protrusions (blebs) form through the flattening of membrane tubes[99,101]. In addition to changes in membrane topography, lipids and proteins in the plasma membrane can diffuse in the plane of the membrane and are mobile, potentially allowing them to reorganize under strain. For example, in supported lipid bilayers recovery of fluorescence occurs within ~20–30 seconds after photobleaching[102], with similar values reported for the recovery of membrane-bound proteins by lateral diffusion and exchange with the cytoplasm in ~20 seconds[103]. It has also been shown that changes in plasma membrane tension following changes in cellular strain coordinates the activation of exocytosis and contraction[104]. In addition to passive effects, mechanical strain has also been suggested to directly affect lipid order and plasma membrane mobility, slowing recovery rates[105]. The plasma membrane is therefore a dynamic cellular structure that can respond to the strains associated with mTBI injury both directly through changes in shape and dynamically through planar diffusion and turnover.

Indeed, changes in membrane morphology are often a hallmark of cellular injury in TBI. For example, Diffuse axonal injury (DAI) is a form of TBI-induced injury characterized by extensive stretch- and shear-induced damage to axonal fibres due to rotational forces experienced during sudden head acceleration or deceleration[106]. Early-stage axonal injuries in DAI are marked by bulging along the long axis of the axons (axonal swelling). Uniaxial stretch experiments on neuronal cells[107] showed that while axons could withstand strain magnitudes of up to 0.65 without severing, they exhibited cytoplasmic and membrane bulging upon returning to their original length (Fig. 3b). Other experiments have reported axonal swellings and the formation of axonal bulbs at strain magnitudes exceeding 0.22 and strain rates over 27 s^{-1}, with these changes becoming more pronounced as strain amplitude and rate increased[108,109]. Pathological axonal membrane swellings where microtubule bundles have disintegrated into loops or waves have been observed in both TBI and neurodegenerative diseases, and highlighting the significance of the interaction between the plasma membrane and underlying cytoskeletal structures[42,107–114]. Interestingly, recent work has also suggested that axonal bulbs may have a protective effect, preventing Ca^{2+} influx into non-stressed regions of the axon[115]. Additionally, axonal injury disrupts fast axonal transport, leading to the abnormal accumulation of amyloid precursor protein (APP) at sites of axonal swelling. This APP buildup, a hallmark of DAI, results from impaired anterograde transport and has been implicated in secondary neurodegenerative processes following TBI[116–118].

In addition to changes in membrane morphology, rupturing of the plasma membrane has also been suggested as a mechanism for axonal injury. Traumatic injury has been shown to increase membrane permeability, which correlates with the rate and magnitude of loading[119–125]. In neuronal injuries, membrane rupture, or the formation of membrane pores under strain (mechanoporation), frequently occurs before neuronal degeneration in tension and shear traumatic brain injury experiments, at strain magnitude of 0.3 and strain rate of 10 s^{-1}[126]. Furthermore, membrane mechanoporation can trigger calcium influx, reactive oxygen species (ROS) generation, and mitochondrial dysfunction, leading to further cellular damage and death[45]. Mechanical stimulation of the membrane is also closely linked with the regulation of mechanosensitive ion channels. Mechanosensitive ion channels, such as Piezo 1 and Piezo2, play a critical role in maintaining neuronal homeostasis by regulating processes like cell migration and differentiation through controlled Ca^{2+} influx[127–130]. Piezo 2 channel in particular helps modulate sensory processes under normal conditions[129,131]. However, TBI conditions can dysregulate Piezo2, leading to an excessive calcium influx. This disruption not only increases cellular stress but also contributes to neuronal death and the production of inflammatory cytokines like TNF-α and IL-1β[132]. For example, cells stretched at strain magnitudes of 0.73–0.9, at a strain rate of 33 s^{-1} exhibited prolonged plasma membrane damage and an increase in cell death (up to 45%), particularly after 12-24 hours post-injury[133].

Microtubules and Axons

Microtubules are cylindrical filaments formed from protofilaments of tubulin dimers and play a critical role in processes such as cell division[134]. Microtubules have a high bending rigidity (i.e. a persistence length of several millimetres[135,136]) and have been reported to have a non-negligible role in determining the mechanical properties of single cells in compression[137–139]. Microtubules are highly dynamic and exhibit dynamic instability, characterized by continuous phases of polymerization and depolymerization (turnover time of 1–10 min)[140,141]. The dynamic behavior of microtubules is regulated by interactions with microtubule-associated proteins (MAPs), which bind to microtubules and influence their stability, dynamics, and cellular interactions. For example, MAP2 serves as a marker of dendritic injury and synaptic plasticity following TBI and has a role in stabilizing microtubules and supporting neuronal structure[142,143]. Similarly, MAP6 (also known as STOP) has been shown to contribute to microtubule stabilization post-TBI[144]. The MAP tau is essential for stabilizing and organizing microtubules in parallel alignment within axons, and the cross-linking of tau helps maintain uniform spacing between adjacent microtubules and reduces depolymerization[145–149]. Axons in neurons are supported by tau-stabilized microtubules, which exhibit a long turnover time of >30 minutes[150,151]. The interplay between turnover dynamics and the mechanical response is particularly significant for microtubules. For example, mechanical stresses have been reported to cause damage to the microtubule lattice, which can repair itself through the addition of new tubulin dimers[152].

In axons, continuous bundles of cross-linked microtubules are thought to provide structural support against different forms of mechanical loading, such as tension and compression[111]. Indeed, mechanical loading can lead to microtubule bending which can lead to internal tension, compression, and shear. This will in turn promote breaking and subsequent depolymerization of microtubules[153,154]. Following loading at a large strain magnitude of 0.3-0.75 and a fixed strain rate of 44 s^{-1}, undulating distortions have been observed to form along axons (Fig. 3c) which coincides with buckling, breakage, and progressive loss of microtubules[42]. Mechanically induced

damage of microtubules and subsequent axonal failure are strain rate dependent[71,155–157], consistent with the notion that bending, potential breakage and disruption of the microtubule network[153,154] occur particularly in regions of the axon where the microtubules are relatively stable with long turnover times.

The strain rate sensitivity of microtubule-based injury may also be attributed to the viscoelastic properties of the neuronal cytoskeleton[158,159]. It has been hypothesised[160] that the tau proteins are viscoelastic: being flexible at low strain rates ($\sim 0.01\ s^{-1}$) allowing for reversible sliding of microtubules[126,161,162] but stiffen up under strain applied at high rate, transferring significant load onto microtubules and potentially causing damage[160]. This microtubular failure likely disrupts neurite transport, leading to an accumulation of vesicles and organelles, which manifests morphologically as axonal beading[163], and causing electrophysiological dysfunction of the neurons[66].

Actin, growth cone, dendrites, and spines

The actin cytoskeleton plays a critical role in determining cell shape and mechanical properties[2,164,165]. Actin filaments are semi-flexible polymers (i.e. a persistence length ~10–20 μm[166]) that assemble into higher order structures such as meshes, bundles, networks and fibres, to enable cells to sustain external load, generate forces, and change shape. The assembly of different actin structures is facilitated by the interaction between actin filaments and an array of regulatory proteins that include actin filament nucleating proteins, crosslinking proteins, and motor proteins[167,168]. All these elements, including actin filaments themselves, are dynamic, allowing cells to dynamically change shape and generate mechanical forces. The turnover timescale of actin filaments and their regulatory proteins is structure dependent and have been measured using fluorescent fusion proteins to actin FRAP. For example, filaments in the actin cortex are highly dynamic, turning over in ~11 seconds[169,170]. By comparison actin filaments and crosslinking proteins in structures such as stress fibres are more stable, taking hundreds of seconds to turn over[171–173]. Interestingly, disease-causing mutations to actin regulatory proteins can lead to excessive polymerization of actin filaments[174,175] or over-crosslinking of actin structures subsequently changing the turnover dynamics of different actin structures and cellular mechanical properties[176,177].

In neurons, actin plays a central role in the formation of distinct structures that are significant for their response to strain loading[178]. In the axon, actin filament rings form along the length of the axon interconnected by spectrin tetramers, with a periodicity of 180-190 nm[179] (Fig. 3d). Actin-spectrin networks have been proposed to have a role in the mechanical response of the axon in TBI. For example, Dubey et. al. [180]. used a custom-built stretching apparatus to investigate the mechanical response of axons to strain loading. They observed that the actin-spectrin cytoskeleton (Fig. 3e) is a prominent contributor to axon mechanics by functioning as a shock absorber. Spectrin proteins are proposed to reversibly unravel[181] by a strain magnitude of up to 0.1, softening the axon and buffering changes in length that could potentially cause damage. In other work, an increase in actin-spectrin spacing from 183 nm to 202 nm has been observed adjacent to neuronal swellings following injury by a strain magnitude of ~0.1[182]. Furthermore, it has been proposed that softening of the spectrin scaffold under repeated mechanical loading exposes microtubules in axons to increased stress during repeated TBI events[183]. In addition to the formation of actin rings in axons, actin plays a critical role in dynamic processes such as the formation of growth cones, dendritic spines, and protrusions. In many of these structures, actin dynamics and remodelling are critical for plasticity and changes in actin dynamics can lead to neurodegenerative disease[184–186]. For example, it has been shown that actin-binding protein cofilin interferes with the actin polymerization process when the cell is subjected to stress, leading to the formation of persistent rod-like structures which are linked to Alzheimer's and Huntington's disease[187–190]. Changes in the turnover dynamics of these disease-associated structures and the corresponding effects on the strain response of these cells is an interesting area of future research.

Conclusion

Traumatic brain injuries (TBI) are a common and significant health concern, with both short- and long-term detrimental effects. Cellular injury in TBI depends on strain magnitude and strain rate, presenting a complex combination of loading conditions. Interestingly, many cell types are able to tolerate high strain magnitudes if loaded at a quasi-static strain rate, but sustain damage from loading applied at high strain rate. This suggests that the turnover of cellular structures, such as the membrane and cytoskeletal polymers, allows cells to adapt to slow physiological loads, but not fast loading. This highlights the significance of considering various mechanical loading parameters (e.g. strain magnitude, strain rate, loading mode, and frequency) in determining cellular and tissue injury. Among these, high strain rate emerges as a critical factor contributing to cellular damage, which can be linked to the mechanical properties and dynamic responses of subcellular structures. In this work, we have introduced some of the key structures that contribute to cellular responses to strain. The plasma membrane, with its rapid turnover time (< 10 s), experiences in-plane tension and serves as a barrier against mechanical deformation. The cytoskeletal components exhibit a range of mechanical responses: actin in the cortex (turnover ~11 s) and stress fibres (> 100 s) primarily counteract tension, while microtubules (1–10 min) and MAP-stabilized microtubules (> 30 min) resist tension, compression, and shear forces. These turnover times highlight the varying capacities of cellular structures to respond to mechanical strain, influencing the extent of injury and potential recovery following traumatic loading. Understanding these behaviours and characteristics is crucial for developing targeted interventions to mitigate cellular damage.

Future research in traumatic brain injury (TBI) should focus on elucidating the interplay between these structural components under different loading conditions, with particular attention to how the dynamics of individual cell components may influence injury thresholds. A possible area of focus could include the study of membrane-cytoskeletal linker proteins and cytoskeletal crosslinking proteins, combined with measurements of their dynamics and mechanical properties, to develop a holistic understanding of cellular injury mechanisms in TBI. Additionally, exploring potential therapeutic strategies to modulate cytoskeletal dynamics and membrane resilience may provide new avenues for mitigating TBI-induced cellular damage. Ultimately, a deeper understanding of these mechanical interactions will enhance our ability to develop effective protective and regenerative strategies in neurotrauma research.

Data Availability

No datasets were generated or analysed during the current study.

Received: 5 February 2025; Accepted: 29 April 2025;
Published online: 03 June 2025

References

1. Chen, C. S. Mechanotransduction–a field pulling together?. *J. cell Sci.* **121**, 3285–3292 (2008).
2. Harris, A. R., Jreij, P. & Fletcher, D. A. Mechanotransduction by the Actin Cytoskeleton: Converting Mechanical Stimuli into Biochemical Signals. *Annu. Rev. Biophys.* **47**, 617–631 (2018).
3. Orr, A. W., Helmke, B. P., Blackman, B. R. & Schwartz, M. A. Mechanisms of mechanotransduction. *Dev. cell* **10**, 11–20 (2006).
4. Barkhausen, T., van Griensven, M., Zeichen, J. & Bosch, U. Modulation of cell functions of human tendon fibroblasts by different repetitive cyclic mechanical stress patterns. *Exp. Toxicol. Pathol.* **55**, 153–158 (2003).
5. Takei, T. et al. Effect of strain on human keratinocytes in vitro. *J. Cell. Physiol.* **173**, 64–72 (1997).
6. Szczodry, M. et al. Treadmill Running Exercise Results in the Presence of Numerous Myofibroblasts in Mouse Patellar Tendons. *J. Orthop. Res.* **27**, 1373–1378 (2009).

7. Fawcett, J. W. & Asher, R. A. The glial scar and central nervous system repair. *Brain Res Bull.* **49**, 377–391 (1999).
8. McGraw, J., Hiebert, G. W. & Steeves, J. D. Modulating astrogliosis after neurotrauma. *J. Neurosci. Res* **63**, 109–115 (2001).
9. Eisenhoffer, G. T. et al. Crowding induces live cell extrusion to maintain homeostatic cell numbers in epithelia. *Nature* **484**, 546–549 (2012).
10. Mammoto, A., Mammoto, T. & Ingber, D. E. Mechanosensitive mechanisms in transcriptional regulation. *J. Cell Sci.* **125**, 3061–3073 (2012).
11. Wagh, K. et al. Mechanical Regulation of Transcription: Recent Advances. *Trends Cell Biol.* **31**, 457–472 (2021).
12. Finch-Edmondson, M. & Sudol, M. Framework to function: mechanosensitive regulators of gene transcription. *Cell. Mol. Biol. Lett.* **21**, 28 (2016).
13. Dupont, S. & Wickström, S. A. Mechanical regulation of chromatin and transcription. *Nat. Rev. Genet* **23**, 624–643 (2022).
14. Humphrey, J. D., Dufresne, E. R. & Schwartz, M. A. Mechanotransduction and extracellular matrix homeostasis. *Nat. Rev. Mol. Cell Biol.* **15**, 802–812 (2014).
15. Oikawa, S. Y., Holloway, T. M. & Phillips, S. M. The Impact of Step Reduction on Muscle Health in Aging: Protein and Exercise as Countermeasures. *Front. Nutr*. **6**, (2019).
16. Bergmann, P. et al. Loading and Skeletal Development and Maintenance. *J. Osteoporos.* **2011**, 786752 (2010).
17. Syková, E. & Nicholson, C. Diffusion in brain extracellular space. *Physiol. Rev.* **88**, 1277–1340 (2008).
18. Duque, J. et al. Rupture strength of living cell monolayers. *Nat. Mater.* 1–12 (2024).
19. Al-Mufti, F. et al. Traumatic brain injury and intracranial hemorrhage–induced cerebral vasospasm: a systematic review. *Neurosurg. focus* **43**, E14 (2017).
20. Coulombe, P. A., Kerns, M. L. & Fuchs, E. Epidermolysis bullosa simplex: a paradigm for disorders of tissue fragility. *J. Clin. Investig.* **119**, 1784–1793 (2009).
21. Cullen, D. K., Simon, C. M. & LaPlaca, M. C. Strain rate-dependent induction of reactive astrogliosis and cell death in three-dimensional neuronal–astrocytic co-cultures. *Brain Res.* **1158**, 103–115 (2007).
22. Fulda, S., Gorman, A. M., Hori, O. & Samali, A. Cellular Stress Responses: Cell Survival and Cell Death. *Int. J. Cell Biol.* **2010**, e214074 (2010).
23. Gefen, A., van Nierop, B., Bader, D. L. & Oomens, C. W. Strain-time cell-death threshold for skeletal muscle in a tissue-engineered model system for deep tissue injury. *J. Biomech.* **41**, 2003–2012 (2008).
24. Kearney, E. M., Prendergast, P. J. & Campbell, V. A. Mechanisms of Strain-Mediated Mesenchymal Stem Cell Apoptosis. *J. Biomech. Engineer.* **130**, 061004 (2008).
25. Quan, X. et al. Mechanical compression insults induce nanoscale changes of membrane-skeleton arrangement which could cause apoptosis and necrosis in dorsal root ganglion neurons. *Biosci. Biotechnol. Biochem* **78**, 1631–1639 (2014).
26. Takano, K. J., Takano, T., Yamanouchi, Y. & Satou, T. Pressure-Induced Apoptosis in Human Lymphoblasts. *Exp. Cell Res.* **235**, 155–160 (1997).
27. Eskandari, F., Shafieian, M., Aghdam, M. M. & Laksari, K. Morphological changes in glial cells arrangement under mechanical loading: A quantitative study. *Injury* **53**, 3617–3623 (2022).
28. Estrada, J. B., Cramer, H. C., Scimone, M. T., Buyukozturk, S. & Franck, C. Neural cell injury pathology due to high-rate mechanical loading. *Brain Multiphys.* **2**, 100034 (2021).
29. Zhu, Y. et al. Mechanical stress influences the morphology and function of human uterosacral ligament fibroblasts and activates the p38 MAPK pathway. *Int Urogynecol. J.* **33**, 2203–2212 (2022).
30. James, S. L. & Theadom, A. Global, regional, and national burden of traumatic brain injury and spinal cord injury, 1990–2016: a systematic analysis for the Global Burden of Disease Study 2016. *Lancet Neurol.* **18**, 56–87 (2019).
31. Langer, L., Levy, C. & Bayley, M. Increasing incidence of concussion: true epidemic or better recognition?. *J. head. trauma Rehabilit.***35**, E60–E66 (2020).
32. Rapp, P. et al. Patient Characterization Protocols for Psychophysiological Studies of Traumatic Brain Injury and Post-TBI Psychiatric Disorders. *Front. Neurol.* **4**, 91 (2013).
33. Silverberg, N. D. & Iverson, G. L. Etiology of the post-concussion syndrome: Physiogenesis and Psychogenesis revisited. *NeuroRehabilitation* **29**, 317–329 (2011).
34. Ryan, L. M. & Warden, D. L. Post concussion syndrome. *Int Rev. Psychiatry* **15**, 310–316 (2003).
35. O'Neil, M. E. et al. Table A-1, Classification of TBI Severity. https://www.ncbi.nlm.nih.gov/books/NBK189784/table/appc.t1/ (2013).
36. Budday, S. et al. Mechanical characterization of human brain tissue. *Acta Biomaterialia* **48**, 319–340 (2017).
37. Giordano, C., Zappalà, S. & Kleiven, S. Anisotropic finite element models for brain injury prediction: the sensitivity of axonal strain to white matter tract inter-subject variability. *Biomech. Model. Mechanobiol.* **16**, 1269–1293 (2017).
38. Wu, T., Alshareef, A., Giudice, J. S. & Panzer, M. B. Explicit modeling of white matter axonal fiber tracts in a finite element brain model. *Ann. Biomed. Eng.* **47**, 1908–1922 (2019).
39. Hajiaghamemar, M. & Margulies, S. S. Multi-scale white matter tract embedded brain finite element model predicts the location of traumatic diffuse axonal injury. *J. Neurotrauma* **38**, 144–157 (2021).
40. Zhou, Z., Olsson, C., Gasser, T. C., Li, X. & Kleiven, S. The white matter fiber tract deforms most in the perpendicular direction during in vivo volunteer impacts. *J. Neurotrauma* **41**, 2554–2570 (2024).
41. Harris, A. R. et al. Characterizing the mechanics of cultured cell monolayers. *Proc. Natl. Acad. Sci.* **109**, 16449–16454 (2012).
42. Tang-Schomer, M. D., Patel, A. R., Baas, P. W. & Smith, D. H. Mechanical breaking of microtubules in axons during dynamic stretch injury underlies delayed elasticity, microtubule disassembly, and axon degeneration. *FASEB J.* **24**, 1401–1410 (2010).
43. Valon, L. & Levayer, R. Dying under pressure: cellular characterisation and in vivo functions of cell death induced by compaction. *Biol. Cell* **111**, 51–66 (2019).
44. Wall, M. E., Weinhold, P. S., Siu, T., Brown, T. D. & Banes, A. J. Comparison of cellular strain with applied substrate strain in vitro. *J. Biomech.* **40**, 173–181 (2007).
45. Wang, F., Franco, R., Skotak, M., Hu, G. & Chandra, N. Mechanical stretch exacerbates the cell death in SH-SY5Y cells exposed to paraquat: mitochondrial dysfunction and oxidative stress. *Neurotoxicology* **41**, 54–63 (2014).
46. Yap, Y. C. et al. Mild and repetitive very mild axonal stretch injury triggers cystoskeletal mislocalization and growth cone collapse. *PloS one* **12**, e0176997 (2017).
47. Gorfinkiel, N., Blanchard, G. B., Adams, R. J. & Martinez Arias, A. Mechanical control of global cell behaviour during dorsal closure in Drosophila. *Development* **136**, 1889–98 (2009).
48. Gorfinkiel, N., Schamberg, S. & Blanchard, G. B. Integrative approaches to morphogenesis: lessons from dorsal closure. *genesis* **49**, 522–533 (2011).
49. Bhattacharya, D., Zhong, J., Tavakoli, S., Kabla, A. & Matsudaira, P. Strain maps characterize the symmetry of convergence and extension patterns during zebrafish gastrulation. *Sci. Rep.* **11**, 19357 (2021).
50. Denberg, D. et al. Computing whole embryo strain maps during gastrulation. *Biophys. J.* **123**, 3911–3922 (2024).
51. Blanchard, G. B. et al. Tissue tectonics: morphogenetic strain rates, cell shape change and intercalation. *Nat. Methods* **6**, 458–464 (2009).
52. He, Z., Ritchie, J., Grashow, J. S., Sacks, M. S. & Yoganathan, A. P. In Vitro Dynamic Strain Behavior of the Mitral Valve Posterior Leaflet. *J. Biomech. Eng.* **127**, 504–511 (2005).

53. Perlman, C. E. & Bhattacharya, J. Alveolar expansion imaged by optical sectioning microscopy. *J. Appl Physiol. ((1985))* **103**, 1037–1044 (2007).
54. Padala, M. et al. Mechanics of the mitral valve strut chordae insertion region. *J. Biomech. Eng.* **132**, 081004 (2010).
55. Maiti, R. et al. In vivo measurement of skin surface strain and sub-surface layer deformation induced by natural tissue stretching. *J. Mech. Behav. Biomed. Mater.* **62**, 556–569 (2016).
56. Waters, C. M., Roan, E. & Navajas, D. Mechanobiology in lung epithelial cells: measurements, perturbations, and responses. *Compr. Physiol.* **2**, 1–29 (2012).
57. Sacks, M. S. et al. Surface Strains in the Anterior Leaflet of the Functioning Mitral Valve. *Ann. Biomed. Eng.* **30**, 1281–1290 (2002).
58. Caporizzo, M. A. & Prosser, B. L. Need for Speed: The Importance of Physiological Strain Rates in Determining Myocardial Stiffness. *Front. Physiol.* **12**, 696694 (2021).
59. Abdi, H., Sanchez-Molina, D., Garcia-Vilana, S. & Rahimi-Movaghar, V. Biomechanical perspectives on traumatic brain injury in the elderly: a comprehensive review. *Prog. Biomed. Eng.* **7**, 022001 (2025).
60. Brett, B. L., Gardner, R. C., Godbout, J., Dams-O'Connor, K. & Keene, C. D. Traumatic Brain Injury and Risk of Neurodegenerative Disorder. *Biol. Psychiatry* **91**, 498–507 (2022).
61. Bain, A. C. & Meaney, D. F. Tissue-level thresholds for axonal damage in an experimental model of central nervous system white matter injury. *J. Biomech. Eng.* **122**, 615–622 (2000).
62. Cater, H. L., Sundstrom, L. E. & Morrison, B. Temporal development of hippocampal cell death is dependent on tissue strain but not strain rate. *J. Biomech.* **39**, 2810–2818 (2006).
63. Margulies, S. S., Thibault, L. E. & Gennarelli, T. A. Physical model simulations of brain injury in the primate. *J. Biomech.* **23**, 823–836 (1990).
64. Meaney, D. F. et al. Biomechanical analysis of experimental diffuse axonal injury. *J. Neurotrauma* **12**, 689–694 (1995).
65. Morrison, B., Cater, H. L., Benham, C. D. & Sundstrom, L. E. An in vitro model of traumatic brain injury utilising two-dimensional stretch of organotypic hippocampal slice cultures. *J. Neurosci. Methods* **150**, 192–201 (2006).
66. Vogel, E. W. et al. Direct Observation of Low Strain, High Rate Deformation of Cultured Brain Tissue During Primary Blast. *Ann. Biomed. Eng.* **48**, 1196–1206 (2020).
67. Morrison, B. et al. A tissue level tolerance criterion for living brain developed with an in vitro model of traumatic mechanical loading. *Stapp car crash J.* **47**, 93–105 (2003).
68. Pfister, B. J., Weihs, T. P., Betenbaugh, M. & Bao, G. An In Vitro Uniaxial Stretch Model for Axonal Injury. *Ann. Biomed. Eng.* **31**, 589–598 (2003).
69. Morrison, B., Elkin, B. S., Dollé, J.-P. & Yarmush, M. L. In Vitro Models of Traumatic Brain Injury. *Annu. Rev. Biomed. Eng.* **13**, 91–126 (2011).
70. Rovt, J., Xu, S., Dutrisac, S., Ouellet, S. & Petel, O. A technique for in situ intracranial strain measurement within a helmeted deformable headform. *J. Mech. Behav. Biomed. Mater.* **147**, 106140 (2023).
71. Panzer, M. B., Myers, B. S., Capehart, B. P. & Bass, C. R. Development of a Finite Element Model for Blast Brain Injury and the Effects of CSF Cavitation. *Ann. Biomed. Eng.* **40**, 1530–1544 (2012).
72. Singh, D., Cronin, D. S. & Haladuick, T. N. Head and brain response to blast using sagittal and transverse finite element models. *Int. J. Numer. Methods Biomed. Eng.* **30**, 470–489 (2014).
73. Bighi, B. et al. Cell stretching devices integrated with live cell imaging: a powerful approach to study how cells react to mechanical cues. *Prog. Biomed. Eng.* **7**, https://doi.org/10.1088/2516-1091/ad9699 (2024).
74. Carpi, N. & Piel, M. Stretching micropatterned cells on a PDMS membrane. *JoVE (Journal of Visualized Experiments)* e51193 (2014).
75. Constantinou, I. & Bastounis, E. E. Cell-stretching devices: advances and challenges in biomedical research and live-cell imaging. *Trends Biotechnol.* **41**, 939–950 (2023).
76. Kah, D. et al. A low-cost uniaxial cell stretcher for six parallel wells. *HardwareX* **9**, e00162 (2021).
77. Kamble, H., Barton, M. J., Jun, M., Park, S. & Nguyen, N.-T. Cell stretching devices as research tools: engineering and biological considerations. *Lab a Chip* **16**, 3193–3203 (2016).
78. Delgado, D., Desroches, S., Kang, G., Aldabii, Y. & Harris, A. R. An Open-Source Combined Atomic Force Microscope and Optical Microscope for Mechanobiology Studies. *Heliyon* **10**, e38214 (2024).
79. Viljoen, A. et al. Force spectroscopy of single cells using atomic force microscopy. *Nat. Rev. Methods Prim.* **1**, 63 (2021).
80. Hochmuth, R. M. Micropipette aspiration of living cells. *J. Biomech.* **33**, 15–22 (2000).
81. Zhang, H. & Liu, K.-K. Optical tweezers for single cells. *J. R. Soc. interface* **5**, 671–690 (2008).
82. Ouyang, H., Nauman, E. & Shi, R. Contribution of cytoskeletal elements to the axonal mechanical properties. *J. Biol. Eng.* **7**, 1–8 (2013).
83. Rotsch, C. & Radmacher, M. Drug-induced changes of cytoskeletal structure and mechanics in fibroblasts: an atomic force microscopy study. *Biophys. J.* **78**, 520–535 (2000).
84. Wu, H. W., Kuhn, T. & Moy, V. T. Mechanical properties of L929 cells measured by atomic force microscopy: effects of anticytoskeletal drugs and membrane crosslinking. *Scanning.: J. Scanning. Microscopies* **20**, 389–397 (1998).
85. Diz-Muñoz, A. et al. Membrane tension acts through PLD2 and mTORC2 to limit actin network assembly during neutrophil migration. *PLoS Biol.* **14**, e1002474 (2016).
86. Moo, E. K. et al. The properties of chondrocyte membrane reservoirs and their role in impact-induced cell death. *Biophys. J.* **105**, 1590–1600 (2013).
87. Lelek, M. et al. Single-molecule localization microscopy. *Nat. Rev. Methods Prim.* **1**, 1–27 (2021).
88. Sauer, M. & Heilemann, M. Single-molecule localization microscopy in eukaryotes. *Chem. Rev.* **117**, 7478–7509 (2017).
89. Elson, E. L. Fluorescence correlation spectroscopy: past, present, future. *Biophys. J.* **101**, 2855–2870 (2011).
90. Krichevsky, O. & Bonnet, G. Fluorescence correlation spectroscopy: the technique and its applications. *Rep. Prog. Phys.* **65**, 251 (2002).
91. Axelrod, D., Koppel, D. E., Schlessinger, J., Elson, E. & Webb, W. W. Mobility measurement by analysis of fluorescence photobleaching recovery kinetics. *Biophys. J.* **16**, 1055–1069 (1976).
92. McNally, J. G. Quantitative FRAP in analysis of molecular binding dynamics in vivo. *Methods cell Biol.* **85**, 329–351 (2008).
93. Reits, E. A. & Neefjes, J. J. From fixed to FRAP: measuring protein mobility and activity in living cells. *Nat. cell Biol.* **3**, E145 (2001).
94. Sprague, B. L. & McNally, J. G. FRAP analysis of binding: proper and fitting. *Trends cell Biol.* **15**, 84–91 (2005).
95. Ammendolia, D. A., Bement, W. M. & Brumell, J. H. Plasma membrane integrity: implications for health and disease. *BMC Biol.* **19**, 1–29 (2021).
96. Andrews, N. W. & Corrotte, M. Plasma membrane repair. *Curr. Biol.* **28**, R392–R397 (2018).
97. Bretscher, M. S. & Raff, M. C. Mammalian plasma membranes. *Nature* **258**, 43–49 (1975).
98. Kwok, R. & Evans, E. Thermoelasticity of large lecithin bilayer vesicles. *Biophys. J.* **35**, 637–652 (1981).
99. Lavi, I. et al. Cellular blebs and membrane invaginations are coupled through membrane tension buffering. *Biophys. J.* **117**, 1485–1495 (2019).
100. Sinha, B. et al. Cells respond to mechanical stress by rapid disassembly of caveolae. *Cell* **144**, 402–413 (2011).

101. Goudarzi, M. et al. Bleb expansion in migrating cells depends on supply of membrane from cell surface invaginations. *Dev. Cell* **43**, 577–587.e5 (2017).
102. Pincet, F. et al. FRAP to characterize molecular diffusion and interaction in various membrane environments. *PloS One* **11**, e0158457 (2016).
103. Goehring, N. W., Chowdhury, D., Hyman, A. A. & Grill, S. W. FRAP analysis of membrane-associated proteins: lateral diffusion and membrane-cytoplasmic exchange. *Biophys. J.* **99**, 2443–2452 (2010).
104. Gauthier, N. C., Fardin, M. A., Roca-Cusachs, P. & Sheetz, M. P. Temporary increase in plasma membrane tension coordinates the activation of exocytosis and contraction during cell spreading. *Proc. Natl. Acad. Sci. USA* **108**, 14467–14472 (2011).
105. Verstraeten, S. V., Mackenzie, G. G. & Oteiza, P. I. The plasma membrane plays a central role in cells response to mechanical stress. *Biochim. Et. Biophys. Acta (BBA)-Biomembranes* **1798**, 1739–1749 (2010).
106. Johnson, V. E., Stewart, W. & Smith, D. H. Axonal pathology in traumatic brain injury. *Exp. Neurol.* **246**, 35–43 (2013).
107. Smith, D. H., Wolf, J. A., Lusardi, T. A., Lee, V. M. & Meaney, D. F. High tolerance and delayed elastic response of cultured axons to dynamic stretch injury. *J. Neurosci.* **19**, 4263–4269 (1999).
108. Aomura, S., Nakadate, H., Kaneko, Y., Nishimura, A. & Willinger, R. Stretch-induced functional disorder of axonal transport in the cultured rat cortex neuron. *Integr. Mol. Med* **3**, 654–660 (2016).
109. Kurtoglu, E., Nakadate, H., Kikuta, K., Aomura, S. & Kakuta, A. Uniaxial stretch-induced axonal injury thresholds for axonal dysfunction and disruption and strain rate effects on thresholds for mouse neuronal stem cells. *JBSE* **12**, 16–00598-16–00598 (2017).
110. Denton, K. R. et al. Loss of spastin function results in disease-specific axonal defects in human pluripotent stem cell-based models of hereditary spastic paraplegia. *Stem Cells* **32**, 414–423 (2014).
111. Hahn, I., Voelzmann, A., Liew, Y.-T., Costa-Gomes, B. & Prokop, A. The model of local axon homeostasis - explaining the role and regulation of microtubule bundles in axon maintenance and pathology. *Neural Dev.* **14**, 11 (2019).
112. Havlicek, S. et al. Gene dosage-dependent rescue of HSP neurite defects in SPG4 patients' neurons. *Hum. Mol. Genet* **23**, 2527–2541 (2014).
113. Sorbara, C. D. et al. Pervasive Axonal Transport Deficits in Multiple Sclerosis Models. *Neuron* **84**, 1183–1190 (2014).
114. Wu, Y.-T., Gilpin, K. & Adnan, A. Effects of Focal Axonal Swelling Level on the Action Potential Signal Transmission. *J. Comput Neurosci.* **48**, 253–263 (2020).
115. Pan, X. et al. Actomyosin-II protects axons from degeneration induced by mild mechanical stress. *J. Cell Biol.* **223**, e202206046 (2024).
116. Itoh, T. et al. Expression of amyloid precursor protein after rat traumatic brain injury. *Neurol. Res.* **31**, 103–109 (2009).
117. Hayashi, T., Ago, K., Nakamae, T., Higo, E. & Ogata, M. Two different immunostaining patterns of beta-amyloid precursor protein (APP) may distinguish traumatic from nontraumatic axonal injury. *Int J. Leg. Med* **129**, 1085–1090 (2015).
118. Romero Tirado, M. A. et al. Beta-amiloid precursor protein (β-App) and diffuse axonal damage after head injuries: a forensic point of view. *Med. Leg. de. Costa Rica* **39**, 37–50 (2022).
119. Farkas, O., Lifshitz, J. & Povlishock, J. T. Mechanoporation Induced by Diffuse Traumatic Brain Injury: An Irreversible or Reversible Response to Injury?. *J. Neurosci.* **26**, 3130–3140 (2006).
120. Geddes, D. M., LaPlaca, M. C. & Cargill, R. S. Susceptibility of hippocampal neurons to mechanically induced injury. *Exp. Neurol.* **184**, 420–427 (2003).
121. Geddes-Klein, D. M., Schiffman, K. B. & Meaney, D. F. Mechanisms and consequences of neuronal stretch injury in vitro differ with the model of trauma. *J. Neurotrauma* **23**, 193–204 (2006).
122. Koob, A. O., Duerstock, B. S., Babbs, C. F., Sun, Y. & Borgens, R. B. Intravenous Polyethylene Glycol Inhibits the Loss of Cerebral Cells after Brain Injury. *J. Neurotrauma* **22**, 1092–1111 (2005).
123. LaPlaca, M. C., LEE, V. M.-Y. & Thibault, L. E. An in vitro model of traumatic neuronal injury: loading rate-dependent changes in acute cytosolic calcium and lactate dehydrogenase release. *J. neurotrauma* **14**, 355–368 (1997).
124. Pettus, E. H. & Povlishock, J. T. Characterization of a distinct set of intra-axonal ultrastructural changes associated with traumatically induced alteration in axolemmal permeability. *Brain Res.* **722**, 1–11 (1996).
125. Prado, G. R. & LaPlaca, M. C. Neuronal plasma membrane integrity is transiently disturbed by traumatic loading. *Neurosci. Insights* **15**, 2633105520946090 (2020).
126. Bar-Kochba, E., Scimone, M. T., Estrada, J. B. & Franck, C. Strain and rate-dependent neuronal injury in a 3D in vitro compression model of traumatic brain injury. *Sci. Rep.* **6**, 30550 (2016).
127. Miyamoto, T. et al. Functional Role for Piezo1 in Stretch-evoked Ca2+ Influx and ATP Release in Urothelial Cell Cultures *. *J. Biol. Chem.* **289**, 16565–16575 (2014).
128. Cinar, E. et al. Piezo1 regulates mechanotransductive release of ATP from human RBCs. *Proc. Natl. Acad. Sci.* **112**, 11783–11788 (2015).
129. Szczot, M. et al. PIEZO2 mediates injury-induced tactile pain in mice and humans. *Sci. Transl. Med.* **10**, eaat9892 (2018).
130. Qin, L. et al. Roles of mechanosensitive channel Piezo1/2 proteins in skeleton and other tissues. *Bone Res* **9**, 1–17 (2021).
131. Chesler, A. T. et al. The Role of PIEZO2 in Human Mechanosensation. *N. Engl. J. Med.* **375**, 1355–1364 (2016).
132. Xiao, Y. et al. Piezo2 Contributes to Traumatic Brain Injury by Activating the RhoA/ROCK1 Pathways. *Mol. Neurobiol.* **61**, 7419–7430 (2024).
133. Skotak, M., Wang, F. & Chandra, N. An in vitro injury model for SH-SY5Y neuroblastoma cells: Effect of strain and strain rate. *J. Neurosci. Methods* **205**, 159–168 (2012).
134. Amos, L. A. & Schlieper, D. Microtubules and maps. *Adv. protein Chem.* **71**, 257–298 (2005).
135. Pampaloni, F. et al. Thermal fluctuations of grafted microtubules provide evidence of a length-dependent persistence length. *Proc. Natl. Acad. Sci.* **103**, 10248–10253 (2006).
136. Wisanpitayakorn, P., Mickolajczyk, K. J., Hancock, W. O., Vidali, L. & Tüzel, E. Measurement of the persistence length of cytoskeletal filaments using curvature distributions. *Biophys. J.* **121**, 1813–1822 (2022).
137. Harris, A. R. & Charras, G. T. Experimental validation of atomic force microscopy-based cell elasticity measurements. *Nanotechnology* **22**, 345102 (2011).
138. Ju, R. J. et al. Compression-dependent microtubule reinforcement enables cells to navigate confined environments. *Nat. Cell Biol.* **26**, 1520–1534 (2024).
139. Li, Y. et al. Compressive forces stabilize microtubules in living cells. *Nat. Mater.* **22**, 913–924 (2023).
140. Salmon, E. D., Leslie, R. J., Saxton, W. M., Karow, M. L. & McIntosh, J. R. Spindle microtubule dynamics in sea urchin embryos: analysis using a fluorescein-labeled tubulin and measurements of fluorescence redistribution after laser photobleaching. *J. Cell Biol.* **99**, 2165–2174 (1984).
141. Schulze, E. & Kirschner, M. Microtubule dynamics in interphase cells. *J. Cell Biol.* **102**, 1020–1031 (1986).
142. TAFT, W. C., YANG, K., DIXON, C. E. & HAYES, R. L. Microtubule-Associated Protein 2 Levels Decrease in Hippocampus Following Traumatic Brain Injury. *J. Neurotrauma* **9**, 281–290 (1992).

143. POSMANTUR, R. M. et al. Diminished Microtubule-Associated Protein 2 (MAP2) Immunoreactivity following Cortical Impact Brain Injury. *J. Neurotrauma* **13**, 125–137 (1996).
144. Song, H. et al. Traumatic brain injury recapitulates developmental changes of axons. *Prog. Neurobiol.* **217**, 102332 (2022).
145. Chen, J., Kanai, Y., Cowan, N. J. & Hirokawa, N. Projection domains of MAP2 and tau determine spacings between microtubules in dendrites and axons. *Nature* **360**, 674–677 (1992).
146. Conde, C. & Cáceres, A. Microtubule assembly, organization and dynamics in axons and dendrites. *Nat. Rev. Neurosci.* **10**, 319–332 (2009).
147. Rosenberg, K. J., Ross, J. L., Feinstein, H. E., Feinstein, S. C. & Israelachvili, J. Complementary dimerization of microtubule-associated tau protein: Implications for microtubule bundling and tau-mediated pathogenesis. *Proc. Natl. Acad. Sci.* **105**, 7445–7450 (2008).
148. Ross, J. L., Santangelo, C. D., Makrides, V. & Fygenson, D. K. Tau induces cooperative Taxol binding to microtubules. *Proc. Natl. Acad. Sci. USA* **101**, 12910–12915 (2004).
149. Shahpasand, K. et al. Regulation of Mitochondrial Transport and Inter-Microtubule Spacing by Tau Phosphorylation at the Sites Hyperphosphorylated in Alzheimer's Disease. *J. Neurosci.* **32**, 2430–2441 (2012).
150. Edson, K. J., Lim, S.-S., Borisy, G. G. & Letourneau, P. C. FRAP analysis of the stability of the microtubule population along the neurites of chick sensory neurons. *Cell Motil.* **25**, 59–72 (1993).
151. Li, Y. & Black, M. M. Microtubule assembly and turnover in growing axons. *J. Neurosci.* **16**, 531–544 (1996).
152. Schaedel, L. et al. Microtubules self-repair in response to mechanical stress. *Nat. Mater.* **14**, 1156–1163 (2015).
153. Odde, D. J., Ma, L., Briggs, A. H., DeMarco, A. & Kirschner, M. W. Microtubule bending and breaking in living fibroblast cells. *J. Cell Sci.* **112**, 3283–3288 (1999).
154. Kabir, A. M. R., Sada, K. & Kakugo, A. Breaking of buckled microtubules is mediated by kinesins. *Biochem. Biophys. Res. Commun.* **524**, 249–254 (2020).
155. Wu, Y.-T. & Adnan, A. Damage and Failure of Axonal Microtubule under Extreme High Strain Rate: An In-Silico Molecular Dynamics Study. *Sci. Rep.* **8**, 12260 (2018).
156. Bicek, A. D., Tüzel, E., Kroll, D. M. & Odde, D. J. Analysis of Microtubule Curvature. in *Methods in Cell Biology* 237–268 (Academic Press, 2007).
157. Goeller, J., Wardlaw, A., Treichler, D., O'Bruba, J. & Weiss, G. Investigation of Cavitation as a Possible Damage Mechanism in Blast-Induced Traumatic Brain Injury. *J. Neurotrauma* **29**, 1970–1981 (2012).
158. Rajagopalan, J., Tofangchi, A. & Saif, M. T. A. The Role of Mechanical Tension in Neurons. *MRS Online Proc. Libr.* **1274**, 106 (2010).
159. Rajagopalan, J., Tofangchi, A. & Saif, A. M. T. Drosophila Neurons Actively Regulate Axonal Tension In Vivo. *Biophys. J.* **99**, 3208–3215 (2010).
160. Ahmadzadeh, H., Smith, D. H. & Shenoy, V. B. Viscoelasticity of Tau Proteins Leads to Strain Rate-Dependent Breaking of Microtubules during Axonal Stretch Injury: Predictions from a Mathematical Model. *Biophys. J.* **106**, 1123–1133 (2014).
161. LaPlaca, M. C. & Thibault, L. E. An in vitro traumatic injury model to examine the response of neurons to a hydrodynamically-induced deformation. *Ann. Biomed. Eng.* **25**, 665–677 (1997).
162. Cullen, D. K., Vernekar, V. N. & LaPlaca, M. C. Trauma-Induced Plasmalemma Disruptions in Three-Dimensional Neural Cultures Are Dependent on Strain Modality and Rate. *J. Neurotrauma* **28**, 2219–2233 (2011).
163. Kilinc, D., Gallo, G. & Barbee, K. A. Mechanically-induced membrane poration causes axonal beading and localized cytoskeletal damage. *Exp. Neurol.* **212**, 422–430 (2008).
164. Dominguez, R. & Holmes, K. C. Actin Structure and Function. *Annu Rev. Biophys.* **40**, 169–186 (2011).
165. Fletcher, D. A. & Mullins, R. D. Cell mechanics and the cytoskeleton. *Nature* **463**, 485–492 (2010).
166. Ott, A., Magnasco, M., Simon, A. & Libchaber, A. Measurement of the persistence length of polymerized actin using fluorescence microscopy. *Phys. Rev. E* **48**, R1642 (1993).
167. Michelot, A. & Drubin, D. G. Building distinct actin filament networks in a common cytoplasm. *Curr. Biol.* **21**, R560–R569 (2011).
168. Pollard, T. D. Actin and actin-binding proteins. *Cold Spring Harb. Perspect. Biol.* **8**, a018226 (2016).
169. Fritzsche, M., Lewalle, A., Duke, T., Kruse, K. & Charras, G. Analysis of turnover dynamics of the submembranous actin cortex. *Mol. Biol. Cell* **24**, 757–767 (2013).
170. Mukhina, S., Wang, Y. & Murata-Hori, M. Alpha-Actinin is Required for Tightly Regulated Remodeling of the Actin Cortical Network during Cytokinesis. *Dev. Cell* **13**, 554–565 (2007).
171. Hotulainen, P. & Lappalainen, P. Stress fibers are generated by two distinct actin assembly mechanisms in motile cells. *J. cell Biol.* **173**, 383–394 (2006).
172. Saito, T., Matsunaga, D. & Deguchi, S. Long-term molecular turnover of actin stress fibers revealed by advection-reaction analysis in fluorescence recovery after photobleaching. *PLoS One* **17**, e0276909 (2022).
173. Skamrahl, M., Colin-York, H., Barbieri, L. & Fritzsche, M. Simultaneous quantification of the interplay between molecular turnover and cell mechanics by AFM–FRAP. *Small* **15**, 1902202 (2019).
174. Albert, M. H. et al. X-linked thrombocytopenia (XLT) due to WAS mutations: clinical characteristics, long-term outcome, and treatment options. *Blood, J. Am. Soc. Hematol.* **115**, 3231–3238 (2010).
175. Moulding, D. A. et al. Excess F-actin mechanically impedes mitosis leading to cytokinesis failure in X-linked neutropenia by exceeding Aurora B kinase error correction capacity. *Blood, J. Am. Soc. Hematol.* **120**, 3803–3811 (2012).
176. Feng, D. et al. Disease-causing mutation in α-actinin-4 promotes podocyte detachment through maladaptation to periodic stretch. *Proc. Natl. Acad. Sci.* **115**, 1517–1522 (2018).
177. Harris, A. R. et al. Steric regulation of tandem calponin homology domain actin-binding affinity. *Mol. Biol. cell* **30**, 3112–3122 (2019).
178. Gallo, G. The Axonal Actin Filament Cytoskeleton: Structure, Function, and Relevance to Injury and Degeneration. *Mol. Neurobiol.*1–19 (2024).
179. Xu, K., Zhong, G. & Zhuang, X. Actin, spectrin, and associated proteins form a periodic cytoskeletal structure in axons. *Science* **339**, 452–456 (2013).
180. Dubey, S. et al. The axonal actin-spectrin lattice acts as a tension buffering shock absorber. *Elife* **9**, e51772 (2020).
181. Hossain, M. N. B. & Adnan, A. Mechanical characterization of spectrin at the molecular level. *Sci. Rep.* **14**, 16631 (2024).
182. Pozo Devoto, V. M. et al. Unraveling axonal mechanisms of traumatic brain injury. *Acta Neuropathol. Commun.* **10**, 140 (2022).
183. Kant, A. et al. Modeling links softening of myelin and spectrin scaffolds of axons after a concussion to increased vulnerability to repeated injuries. *Proc. Natl. Acad. Sci.* **118**, e2024961118 (2021).
184. Ben Zablah, Y., Merovitch, N. & Jia, Z. The Role of ADF/Cofilin in Synaptic Physiology and Alzheimer's Disease. *Front. Cell Dev. Biol*. **8**, 594998 (2020).
185. Borovac, J., Bosch, M. & Okamoto, K. Regulation of actin dynamics during structural plasticity of dendritic spines: Signaling messengers and actin-binding proteins. *Mol. Cell. Neurosci.* **91**, 122–130 (2018).
186. Lamprecht, R. Actin Cytoskeleton Role in the Maintenance of Neuronal Morphology and Long-Term Memory. *Cells* **10**, 1795 (2021).

187. Cichon, J. et al. Cofilin Aggregation Blocks Intracellular Trafficking and Induces Synaptic Loss in Hippocampal Neurons*. *J. Biol. Chem.* **287**, 3919–3929 (2012).
188. Minamide, L. S., Striegl, A. M., Boyle, J. A., Meberg, P. J. & Bamburg, J. R. Neurodegenerative stimuli induce persistent ADF/cofilin–actin rods that disrupt distal neurite function. *Nat. Cell Biol.* **2**, 628–636 (2000).
189. Nishida, E. et al. Cofilin is a component of intranuclear and cytoplasmic actin rods induced in cultured cells. *Proc. Natl. Acad. Sci.* **84**, 5262–5266 (1987).
190. Ohta, Y., Nishida, E., Sakai, H. & Miyamoto, E. Dephosphorylation of cofilin accompanies heat shock-induced nuclear accumulation of cofilin. *J. Biol. Chem.* **264**, 16143–16148 (1989).
191. Burr, D. B. et al. In vivo measurement of human tibial strains during vigorous activity. *Bone* **18**, 405–410 (1996).
192. Carretta, R. et al. Novel method to analyze post-yield mechanical properties at trabecular bone tissue level. *J. Mech. Behav. Biomed. Mater.* **20**, 6–18 (2013).
193. Lanyon, L. E., Hampson, W. G., Goodship, A. E. & Shah, J. S. Bone deformation recorded in vivo from strain gauges attached to the human tibial shaft. *Acta Orthop. Scand.* **46**, 256–268 (1975).
194. Morgan, E. F., Unnikrisnan, G. U. & Hussein, A. I. Bone Mechanical Properties in Healthy and Diseased States. *Annu Rev. Biomed. Eng.* **20**, 119–143 (2018).
195. Turunen, M. J. et al. Sub-trabecular strain evolution in human trabecular bone. *Sci. Rep.* **10**, 13788 (2020).
196. Polio, S. R. et al. Cross-platform mechanical characterization of lung tissue. *PLOS ONE* **13**, e0204765 (2018).
197. Protti, A. et al. Role of Strain Rate in the Pathogenesis of Ventilator-Induced Lung Edema. *Crit. Care Med.* **44**, e838 (2016).
198. Bates, N. A., Schilaty, N. D., Nagelli, C. V., Krych, A. J. & Hewett, T. E. Validation of Non-Contact Anterior Cruciate Ligament Tears Produced by a Mechanical Impact Simulator Against the Clinical Presentation of Injury. *Am. J. Sports Med.* **46**, 2113–2121 (2018).
199. Karunaratne, A., Li, S. & Bull, A. M. J. Nano-scale mechanisms explain the stiffening and strengthening of ligament tissue with increasing strain rate. *Sci. Rep.* **8**, 3707 (2018).
200. Sanchez-Adams, J., Leddy, H. A., McNulty, A. L., O'Conor, C. J. & Guilak, F. The Mechanobiology of Articular Cartilage: Bearing the Burden of Osteoarthritis. *Curr. Rheumatol. Rep.* **16**, 451 (2014).
201. Vogel, E. W., Rwema, S. H., Meaney, D. F., Bass, C. R. D. & Morrison, B. Primary Blast Injury Depressed Hippocampal Long-Term Potentiation through Disruption of Synaptic Proteins. *J. Neurotrauma* **34**, 1063–1073 (2017).
202. Esfahani, A. M. et al. Characterization of the strain-rate–dependent mechanical response of single cell–cell junctions. *Proc. Natl. Acad. Sci.* **118**, e2019347118 (2021).
203. Tahaei, A. et al. Cell divisions imprint long lasting elastic strain fields in epithelial tissues. Preprint at http://arxiv.org/abs/2406.03433 (2024).
204. Cox, B. N. & Smith, D. W. On strain and stress in living cells. *J. Mech. Phys. Solids* **71**, 239–252 (2014).
205. Young, H. M. et al. Dynamics of neural crest-derived cell migration in the embryonic mouse gut. *Dev. Biol.* **270**, 455–473 (2004).
206. Power, R. E. et al. Mechanical Deformation Induced Apoptosis in Human Proximal Renal Tubular Epithelial Cells is Caspase Dependent. *J. Urol.* **171**, 457–461 (2004).
207. Gladman, S. J., Ward, R. E., Michael-Titus, A. T., Knight, M. M. & Priestley, J. V. The effect of mechanical strain or hypoxia on cell death in subpopulations of rat dorsal root ganglion neurons in vitro. *Neuroscience* **171**, 577–587 (2010).
208. Yano, S., Komine, M., Fujimoto, M., Okochi, H. & Tamaki, K. Mechanical Stretching In Vitro Regulates Signal Transduction Pathways and Cellular Proliferation in Human Epidermal Keratinocytes. *J. Invest Dermatol* **122**, 783–790 (2004).
209. Engel, D. C., Slemmer, J. E., Vlug, A. S., Maas, A. I. R. & Weber, J. T. Combined effects of mechanical and ischemic injury to cortical cells: Secondary ischemia increases damage and decreases effects of neuroprotective agents. *Neuropharmacology* **49**, 985–995 (2005).

Acknowledgements

This research received financial support from the Department of the Army, U.S. Army Research Office under contract W911NF-23-1-0390. A.R.H. gratefully acknowledges support from NSERC (RGPIN-2022-04933) and the Banting Foundation Discovery award program. E.K.M. would like to thank NSERC Discovery Program (RGPIN-2023-05127) and Carleton University (grant numbers 186725, 187023, 186984) for their financial support.

Author contributions

G.K., E.K.M, O.E.P, and A.R.H. contributed to writing, reviewing and editing. R.B. contributed to reviewing and editing. All authors approved the completed version of the manuscript and are accountable for the work.

Competing interests

The authors declare no competing interests.

Additional information

Correspondence and requests for materials should be addressed to Andrew R. Harris.